



**CHALMERS**  
UNIVERSITY OF TECHNOLOGY

## **Plasmonic Hydrogen Sensing with Nanostructured Metal Hydrides**

Downloaded from: <https://research.chalmers.se>, 2024-08-17 06:35 UTC

Citation for the original published paper (version of record):

Wadell, C., Syrenova, S., Langhammer, C. (2014). Plasmonic Hydrogen Sensing with Nanostructured Metal Hydrides. *ACS Nano*, 8(12): 11925-11940. <http://dx.doi.org/10.1021/nm505804f>

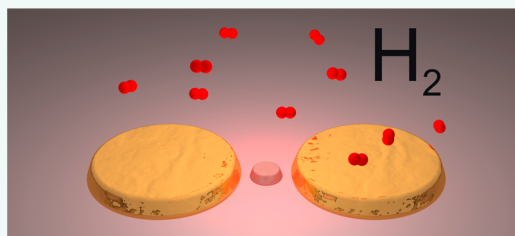
N.B. When citing this work, cite the original published paper.

# Plasmonic Hydrogen Sensing with Nanostructured Metal Hydrides

Carl Wadell, Svetlana Syrenova, and Christoph Langhammer\*

Department of Applied Physics, Chalmers University of Technology, 412 96 Göteborg, Sweden

**ABSTRACT** In this review, we discuss the evolution of localized surface plasmon resonance and surface plasmon resonance hydrogen sensors based on nanostructured metal hydrides, which has accelerated significantly during the past 5 years. We put particular focus on how, conceptually, plasmonic resonances can be used to study metal–hydrogen interactions at the nanoscale, both at the ensemble and at the single-nanoparticle level. Such efforts are motivated by a fundamental interest in understanding the role of nanosizing on metal hydride formation processes in the quest to develop efficient solid-state hydrogen storage materials with fast response times, reasonable thermodynamics, and acceptable long-term stability. Therefore, a brief introduction to the thermodynamics of metal hydride formation is also given. However, plasmonic hydrogen sensors not only are of academic interest as research tool in materials science but also are predicted to find more practical use as all-optical gas detectors in industrial and medical applications, as well as in a future hydrogen economy, where hydrogen is used as a carbon free energy carrier. Therefore, the wide range of different plasmonic hydrogen sensor designs already available is reviewed together with theoretical efforts to understand their fundamentals and optimize their performance in terms of sensitivity. In this context, we also highlight important challenges to be addressed in the future to take plasmonic hydrogen sensors from the laboratory to real applications in devices, including poisoning/deactivation of the active materials, sensor lifetime, and cross-sensitivity toward other gas species.



**KEYWORDS:** localized surface plasmon resonance · surface plasmon resonance · hydrogen · sensors · metal hydride · palladium · nanoparticles · nanowires · sensing

Hydrogen is the first chemical element in the periodic table. At ambient temperature and pressure, hydrogen is a colorless, odorless, tasteless, and highly flammable diatomic gas with the molecular formula  $H_2$ . With an atomic weight of 1.00794, hydrogen is the lightest and, by constituting roughly 75% of the present elemental mass, also the most abundant element in the universe. Stars are mainly composed of hydrogen. However, on Earth, elemental hydrogen is relatively rare as it forms compounds with most elements and is present in water and most organic molecules.

In the 1970s, several visionary studies announced a so-called *hydrogen economy*, a scenario where sustainable energy sources convert energy into electricity, which is then used to produce hydrogen from water.<sup>1</sup> The produced hydrogen is subsequently used as energy vector to store and transport the produced energy. At the consumer, the chemical energy stored in the hydrogen gas is converted back into electrical energy in a

fuel cell with only water as byproduct. The water is thus recycled in a closed loop, and no harmful emissions are created.

**Why Do We Need Hydrogen Sensors?** For the hydrogen economy to become reality, the challenge stands in optimizing costs, reliability, and safety at all stages of hydrogen production, distribution, storage, and utilization as a fuel.<sup>2</sup> Thus, hydrogen sensing potentially has an important role to play in several different aspects of this quest. For example, from a materials science perspective, hydrogen sensing turns out to be very useful to generate deeper understanding of material–hydrogen interactions at the nanoscale, which is important for the development of efficient hydrogen storage media. As another example, if hydrogen is introduced as the major energy carrier, hydrogen sensors will become a vital part of the infrastructure to ensure safe operation, that is, to detect hydrogen leaks from storage tanks, gas lines, etc., to prevent ignition/explosion of highly flammable/explosive hydrogen–air mixtures.

\* Address correspondence to clangham@chalmers.se.

Received for review October 11, 2014 and accepted November 26, 2014.

Published online November 26, 2014  
10.1021/nn505804f

© 2014 American Chemical Society

Hydrogen sensors are, however, not only of importance in a future hydrogen economy. Already today hydrogen gas is largely involved in various areas of the chemical industry either being one of the necessary components or by-/end product of chemical processes. In these fields, hydrogen is mainly used in two nonfuel applications such as production of ammonia for the fertilizer industry and refinement of crude oils in the petrochemical industry. For these applications, hydrogen sensors are needed in order to monitor and control hydrogen partial pressure for as safe and as efficient processing as possible.<sup>3</sup>

Besides these applications in the chemical industry, hydrogen sensing can be useful when hydrogen is an end product or byproduct of a biological process. For example, in the food industry, detection of hydrogen produced by certain bacteria can help determine if the food is spoiled.<sup>4</sup> Hydrogen sensing was also suggested to be used for indication of whether the food has been irradiated<sup>5</sup> or for detection of leaks in flexible food packages by employing it as a tracer gas.<sup>6</sup> Also in medical applications, an interest in hydrogen sensors has arisen since measuring the hydrogen content in human breath has proven to be useful to diagnose certain conditions such as lactose intolerance or bacterial overgrowth in intestines.<sup>7</sup>

**What Are the Requirements for Hydrogen Sensors?** Hydrogen sensors have to comply with a number of requirements that can be quite specific depending on application areas. These requirements can be generally summarized<sup>3,8,9</sup> as acceptable measurement range (e.g., 0.01–10% for leak detection—note that the flammability limit for hydrogen–air mixtures is from 4 to 75 vol % H<sub>2</sub>), sufficient accuracy (uncertainty less than 5–10% of signal) and reliability, quick response and recovery time (<1 s), stable signal with good signal-to-noise ratio, robustness under environmental conditions (e.g., temperature (–30 to 80 °C), pressure (80–110 kPa), relative humidity (10–98%)). At the same time, an ideal hydrogen sensor has to be explosion-proof, have long lifetime (>5 years) and low cost, feature simple operation and maintenance as well as simple system integration and interface. Other important characteristics of hydrogen sensors are low cross-sensitivity and low susceptibility to contamination and poisoning toward/by other chemical species, such as hydrocarbons, water, carbon monoxide, hydrogen sulfide, sulfur dioxide, etc.

**Why Optical Hydrogen Sensors?** Several mechanisms for hydrogen sensing have been studied for more than a century. Traditional approaches include gas chromatography, mass spectrometry, thermal conductivity sensors, and laser gas analysis. There are also commercially available sensors based on a solid-state approach to hydrogen sensing such as catalytic sensors, electrochemical sensors, resistance-based sensors, work-function-based sensors, as well as sensors with mechanical, acoustical, and optical readouts.

**Localized surface plasmon resonance** - Resonant collective oscillations of electrons in a nanoparticle that consists of a material that features free electrons, for example, a metal. The resonance condition is established when the frequency of irradiated near-visible light matches the natural frequency of the free electrons oscillating against the restoring force of positive nuclei in the nanoparticle; **Surface plasmon resonance** - Surface electromagnetic waves that propagate parallel to a metal/dielectric or metal/vacuum interface at optical frequencies and that create evanescent fields into the dielectric/vacuum; **Direct nanoplasmonic sensing** - Nanoplasmonic sensing arrangement where the plasmonic antenna constitutes both the active material interacting with the analyte and the plasmonic signal transducer; **Indirect nanoplasmonic sensing** - Nanoplasmonic sensing arrangement where a chemically inert plasmonic antenna located adjacent (within a few to few tens of nanometers) to the active material, interacting with the analyte, acts as plasmonic signal transducer; **Pressure–composition isotherm** - Graphical representation of the hydrogen concentration in a material as a function of applied external hydrogen (partial) pressure at constant temperature;  **$\alpha$ -Phase** - Solid solution of hydrogen atoms in a host material lattice at concentrations low enough to render hydrogen–hydrogen interactions negligible; **Metal hydride** - Compound, also called  $\beta$ -phase, formed by interaction of metals with hydrogen, which often is nonstoichiometric. Binary hydrides contain only two elements, the metal (M) and hydrogen. The bonds formed between hydrogen and metal can vary between ionic, covalent, or metallic, depending on the system. Most transition metal hydrides exhibit metal-like electrical conductivity.

Comprehensive reviews on existing and emerging hydrogen-sensing technologies mentioned above can be found in recent work by Hübert *et al.*<sup>10</sup> Ando<sup>11</sup> also specifically summarizes detection of various gases (including hydrogen) by means of optochemical sensors. Our review is focused on a new family of optical hydrogen sensors that capitalize on the recent advances in nanophotonics and the phenomena of the surface plasmon resonance (SPR) at a metal dielectric interface and the localized surface plasmon resonance (LSPR) in metal nanoparticles. Optical sensors in general have a number of advantages compared to the traditional electrical ones. The main advantage is that they pose no risk to generate sparks, something that could be devastating when operating in explosive hydrogen atmospheres. They also have the benefit of not being affected by electromagnetic interference and feature remote readout, which is attractive in harsh environments.

In order to build an optical hydrogen sensor, some kind of “active” material that specifically reacts in a measurable way to the presence of hydrogen is needed. Numerous different materials that fulfill this criterion exist, such as various metals, metal oxides, and polymers. In this review, we have chosen to focus on the transformation of a metal into a hydride in the

presence of hydrogen<sup>12</sup> as the detection reaction. We make this selection since the plasmon resonance is a phenomenon that occurs in metals and because of the fact that most plasmonic hydrogen sensors demonstrated to date exploit this transformation. For historical completeness, however, we will also include an overview on plasmonic hydrogen sensors utilizing other active materials, such as oxides. These will, however, not be discussed in detail.

The outline of the remainder of this review is as follows. We start out with a brief introduction to the thermodynamics of metal–hydrogen interactions as a background for the sensing principle of metal hydride-based plasmonic gas sensors, followed by a section on the generic principles of plasmonic sensing. After these introductory paragraphs, we will review in detail the fields of LSPR- and SPR-based hydrogen sensors that rely on nanostructured metal hydrides. This is followed by a short section on recent developments of alternative optical concepts, which may prove inspirational to the fields of LSPR- and SPR-based hydrogen sensing. We then sum up by discussing future avenues and challenges for metal hydride-based plasmonic hydrogen sensors, which we feel are critical to further advance the field.

#### THERMODYNAMICS OF THE METAL–HYDROGEN SYSTEM

The ability of metals to absorb hydrogen atoms into interstitial sites in their lattice has received a lot of research attention over the years with different

applications in mind.<sup>12</sup> The main interest is perhaps in application as hydrogen storage medium for on-board storage systems for vehicles, owing to the large volume reduction of the hydrogen when stored in a metal hydride compared to, for instance, a high-pressure gas tank.<sup>13</sup> Nevertheless, we note that, in today's planned pre-series vehicles that feature hydrogen-powered fuel cells, advanced composite material high-pressure gas tanks are used as the hydrogen storage solution because it is the most efficient available technology today.<sup>14</sup> Also, stationary hydrogen storage at a larger scale and metal hydride batteries are important application areas of metal hydrides.<sup>15</sup> In the field, hydride formation in metal nanoparticles has become a hot topic during the recent years as the sorption behavior is expected to differ greatly in nanosized entities compared to their bulk counterparts and thus offers interesting opportunities to engineer the hydrogen storage properties of a material.<sup>16</sup> As mentioned, the metal hydride formation can also be utilized in hydrogen sensors as the “detection reaction”. Thus, to gain some insight into the working principle of such sensors, we first briefly discuss the hydride formation process in a metal (Figure 1).

As the metal is exposed to hydrogen molecules, they dissociate on the metal surface (we note, however, that on many metals this is an activated process that does not occur spontaneously at ambient conditions) and the hydrogen atoms start to diffuse into the metal lattice. At low hydrogen gas pressures, a solid solution of hydrogen in the host lattice (called the  $\alpha$ -phase;

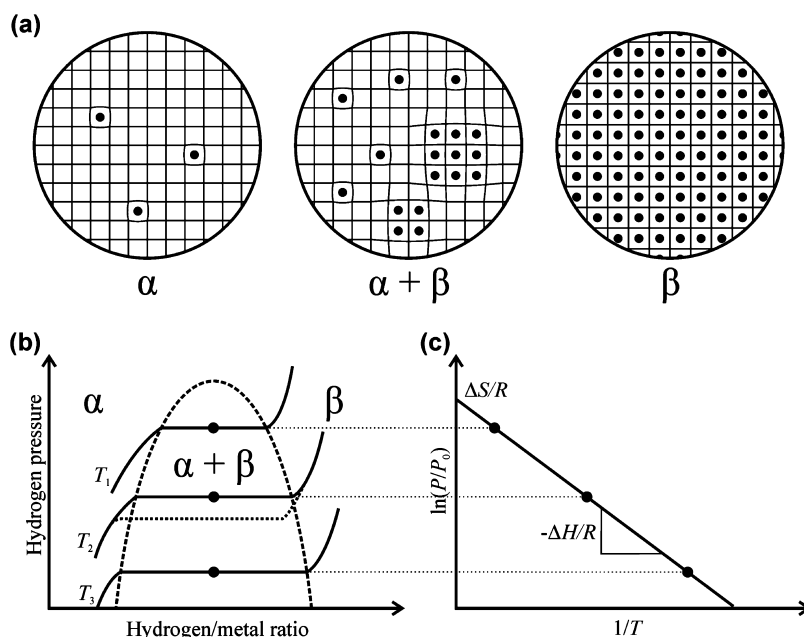


**Figure 1.** Sketch of the hydride formation process in a metal. (a) Different stages during the hydride formation:  $\alpha$ -phase, mixed phase, and fully formed hydride ( $\beta$ -phase). (b) Sketch of pressure–composition isotherms exhibiting a plateau at the hydride formation pressure for a given temperature. This plateau pressure increases as the temperature increases. (c) van't Hoff analysis where changes in enthalpy ( $\Delta H$ ) and entropy ( $\Delta S$ ) during the hydride formation are extracted from the temperature dependence of the plateau pressures.

see Figure 1a) is formed. In this  $\alpha$ -phase, since the amount of hydrogen is rather low and thus the distance between hydrogen atoms is large, (attractive) hydrogen–hydrogen interactions inside the lattice are very weak. Nevertheless, as the metal absorbs more and more hydrogen, it will locally strain the lattice of the host. As the hydrogen pressure/concentration is increased even further, the amount of hydrogen in the metal will increase, and eventually, hydrogen–hydrogen interactions (resulting from lattice strain as well as electronic interactions) become appreciable and the formation of regions of the hydride ( $\beta$ -phase) starts. At this stage, the  $\alpha$ -phase and  $\beta$ -phase coexist in equilibrium, and an incremental increase in the hydrogen concentration around the metal will only result in the growth of the  $\beta$ -phase regions at the expense of the  $\alpha$ -phase. Eventually, with continued increased external hydrogen pressure, the entire metal will be transformed into the  $\beta$ -phase, the hydride formation is complete, and any further increase in hydrogen pressure will only result in minor changes in the hydrogen content in the hydride.

If one—at constant temperature—maps the hydrogen content in the metal *versus* the increasing applied hydrogen pressure, a so-called pressure–composition isotherm is obtained (see Figure 1b). The isotherm exhibits a clear “plateau” at the pressure where the  $\alpha$ - and  $\beta$ -phase coexist, that is, at the hydride formation pressure. As the temperature is increased, the pressure at which the hydride formation takes place also increases. In this way, by measuring isotherms at several temperatures, the phase diagram of the metal–hydrogen system can be mapped out. The phase boundaries are located on the low and high concentration sides of the equilibrium plateau, respectively, and narrow up toward the critical point.

If one now reverses the process and decreases the hydrogen pressure around the hydride, the unloading process will take place in a similar way and exhibit a plateau where  $\beta$ -phase and  $\alpha$ -phase are in thermodynamic equilibrium as the hydride is decomposed. However, the hydride decomposition will in most cases not occur at the same pressure as the formation but rather at lower pressure. This hysteresis is also the result of the lattice strain induced by the presence of hydrogen in the metal lattice. This strain creates an energy barrier that needs to be surmounted in order for the hydride to form or decompose.<sup>17</sup> One way to engineer the extent of the hysteresis is typically to alloy the host metal with a second element, as for example in Pd–Au, Pd–Ag, and Pd–Ni alloys.<sup>18–20</sup>

From isotherm measurements carried out at different temperatures, it is possible to extract thermodynamic data regarding the hydride formation/decomposition process. At the plateau, the chemical potentials of hydrogen in the gas phase and in the hydride phase are equal by definition.<sup>21</sup> This equality

gives rise to the van't Hoff equation:

$$\ln \frac{P}{P_0} = -\frac{\Delta H}{RT} + \frac{\Delta S}{R} \quad (1)$$

where  $P$  is the plateau pressure,  $P_0$  is atmospheric pressure,  $\Delta H$  and  $\Delta S$  are, respectively, the changes in enthalpy and entropy for the hydride formation/decomposition,  $R$  is the gas constant, and  $T$  is the temperature. By measuring pressure–composition isotherms at different temperatures and extracting the plateau pressures, it is thus possible to use the van't Hoff equation to extract  $\Delta H$  and  $\Delta S$ . This is done using a so-called van't Hoff plot in which  $\ln(P/P_0)$  is plotted *versus*  $1/T$  (Figure 1c). From the obtained line,  $\Delta H$  and  $\Delta S$  are determined by the slope of the line and its intersection with the  $y$ -axis, respectively. These are important parameters, in particular  $\Delta H$ , since it quantifies the amount of energy required to release the hydrogen from the hydride (*i.e.*, its thermal stability). For a sensor, this is of particular relevance when it comes to regeneration; that is, it is desirable that the hydride phase spontaneously decomposes at ambient temperature conditions, when the hydrogen concentration in the sensor environment decreases.

## PRINCIPLES OF PLASMONIC SENSING

As light is irradiated on a metal nanoparticle that is smaller or comparable to the wavelength, resonant collective oscillations of the conduction electrons can be excited with respect to the immobilized positive ion cores in the lattice—the localized surface plasmon resonance depicted in Figure 2a. At the wavelength where the resonance occurs, the metal nanoparticles

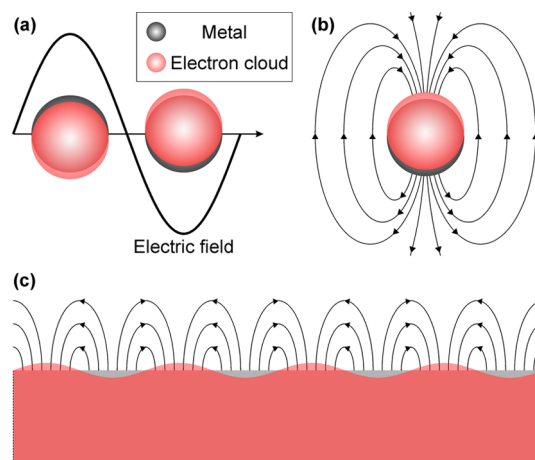


**Figure 2.** (a) Sketch of the localized surface plasmon resonance in a metal nanoparticle as it is subjected to a time-dependent electric field, such as light. (b) Charge separation at the surface of the metal nanoparticle caused by the LSPR generates an enhanced electric field near the nanoparticle. (c) Similar to the nanoparticle case, at the surface of a metal film toward a dielectric or vacuum, a surface plasmon resonance can be excited under the right conditions. Also here the surface charge variations result in an evanescent electric field close to the surface of the metal film.

will strongly absorb and scatter light. This phenomenon was first reported by Faraday in 1857 as he studied coloration of gold nanoparticle colloids.<sup>22</sup> However, the principle had already been used for centuries to stain glass (*e.g.*, church windows). Because of charge separation at the surface of the nanoparticle as the resonance is excited, a strongly enhanced electric field is generated locally around the nanoparticle (see Figure 2b). The wavelength at which the LSPR occurs depends on several factors including the size, shape, and material of the nanoparticle, but it also depends on the environment around it, that is, its dielectric properties.<sup>23</sup> Therefore, by tracking the LSPR wavelength, it is possible to detect any changes to the nanoparticle itself (*via* change of the size/shape or materials/electronic properties) or to its immediate surroundings (*via* change of surrounding dielectric properties). The former sensing principle can be referred to as *direct plasmonic sensing* and the latter one as *indirect plasmonic sensing*, as schematically illustrated in Figure 3.

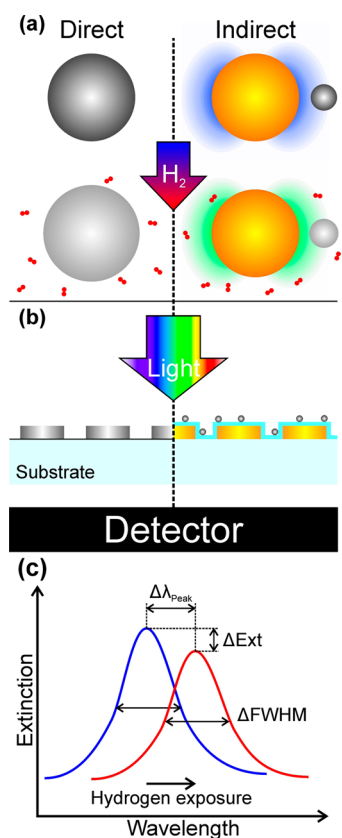


**Figure 3.** Schematic depiction of the working principles of direct and indirect nanoplasmonic sensors. (a) In the direct sensing case, the nanoparticle acts both as active material reacting with hydrogen and as plasmonic signal transducer, whereas in the case of indirect sensing, an inert plasmonic sensor particle is used to probe the interaction of hydrogen with the adjacent active material. (b) LSPR of the sensor is excited by polychromatic light, and scattering or extinction spectra are recorded. (c) By tracking the spectral position, intensity, or line width of the LSPR peak in the recorded spectra, the presence of hydrogen can be detected as characteristic shifts in these readout parameters.

Similarly to the metal nanoparticle case, it is also possible to induce resonant collective electron excitations on metal films at the interface toward a dielectric or toward vacuum (see Figure 2c). On a film, the resonance is no longer localized, as in nanoparticles, but can be understood as a freely propagating surface charge density wave. These resonances are called surface plasmon resonances or surface plasmon polaritons. Because of the charge separation along the surface of the metal, an evanescent electric field will be generated. SPRs can thus be used for sensing in a similar fashion as the LSPRs. However, unlike the LSPRs, SPRs cannot be excited directly by light at normal incidence. The light needs to be provided momentum to excite the SPR, which is most commonly achieved by the use of a prism coupler, a diffraction grating, or a waveguide.<sup>24</sup>

### LSPR METAL HYDRIDE HYDROGEN SENSORS

**Direct LSPR Hydrogen Sensors.** Direct LSPR hydrogen sensors consist of hydride-forming metal nanoparticles, such as Pd. The LSPR of these nanoparticles is utilized to monitor the hydrogen uptake in the metal, hence the name *direct* hydrogen sensing. As hydrogen is absorbed into the metal lattice, it will expand and also the permittivity of the metal will change.<sup>25</sup> These effects will influence the resonance conditions for the LSPR, which is used as the readout of the sensor. The first example of a direct LSPR sensor using a nanostructure hydride is the work by Langhammer *et al.*,<sup>26</sup> where Pd nanodisks on a glass support are used as the sensing platform. In this work, the sensor arrangement was inserted into a vacuum chamber and the hydrogen uptake/release was controlled by varying the pressure of hydrogen gas. The chamber was equipped with windows, making it possible to monitor the LSPR resonance of the sample by a simple transmission measurement. In a later paper by the same authors,<sup>27</sup> this work was extended by also studying the temperature dependence of pressure–composition isotherms to extract thermodynamic information about the system according to the van't Hoff procedure described in the introduction (see Figure 4a). Additionally, to verify that the LSPR shifts in these measurements indeed stem from the hydrogen uptake in the Pd nanoparticles, a quartz crystal microbalance was used to experimentally determine the correlation between hydrogen concentration in the Pd nanodisks and the LSPR peak shift.<sup>27,28</sup> A linear correlation was found for the considered Pd nanodisk sizes and later theoretically verified based on first-principles calculations by Poyli *et al.*<sup>29</sup> Apart from Pd nanodisks, other nanostructures have since then been developed for direct LSPR hydrogen sensing, including Pd nanorings<sup>30</sup> and concave Pd nanocubes.<sup>31</sup> In the work by Strohfeltd *et al.*,<sup>32</sup> these sensors have been

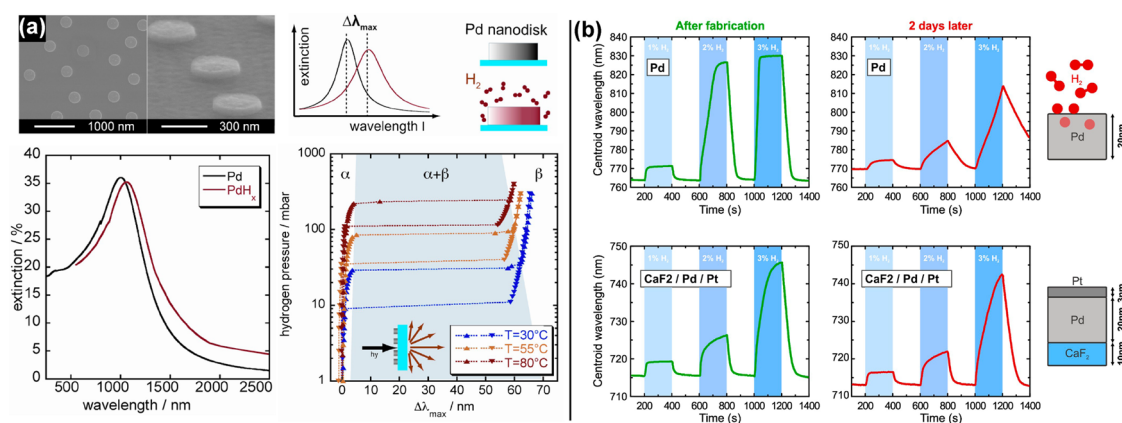


**Figure 4.** (a) Direct sensing of hydrogen sorption in Pd nanodisks. By tracking the shift of the LSPR upon hydrogen exposure, temperature-dependent pressure–composition isotherm measurements can be performed to derive the enthalpy and entropy of hydride formation in the disks. Adapted with permission from ref 27. Copyright 2010 Wiley-VCH Verlag GmbH & Co. KGaA, Weinheim. (b) Long-term stability of a direct plasmonic hydrogen sensor based on hydride formation in Pd. After only 2 days, the sensor's response has deteriorated significantly (top panel). By adding a bottom layer of  $\text{CaF}_2$  and a thin layer of Pt catalyst on top of the Pd nanodisks (bottom panel), the long-term stability of the sensor is significantly enhanced. Adapted with permission from ref 32. Copyright 2013 Optical Society of America.

taken one step further, not only by considering a Pd disk but also by using a layered disk structure consisting of a bottom  $\text{CaF}_2$  layer, a middle Pd layer, and a top Pt cap, as shown in Figure 4b. The addition of these extra layers (Pd still acts as the active material for hydrogen detection) has been shown to have a great impact on the long-term stability of the hydrogen-sensing signal via a “catalytic cleaning” effect of the Pt layer. Efforts in this direction are of vital importance if these types of sensors are to be able to compete with other types of hydrogen sensors in real applications.

The works presented above all feature Pd as the sensing material. Recently, alternative materials have been investigated for their applicability in direct LSPR sensors. Sil *et al.*<sup>33</sup> reported that substrates covered by gold hemispheres in the size range of 20–36 nm show a plasmonic response in the presence of hydrogen. They attribute this plasmonic response to the formation of a metastable gold hydride phase, which becomes possible through hot-electron-induced  $\text{H}_2$  dissociation on the otherwise inert Au surface. This kind of plasmon-induced  $\text{H}_2$  dissociation on Au nanoparticles was first reported by Mukherjee *et al.* in 2012.<sup>34</sup>

In another recent work, Strohfeltdt *et al.*<sup>35</sup> demonstrated that when using yttrium (Y) nanoparticles, it is possible to switch the LSPR on and off by hydrogen exposure. Specifically, as the Y particles are initially exposed to hydrogen, an insulating yttrium trihydride ( $\text{YH}_3$ ) is formed, efficiently suppressing the LSPR. As the hydrogen gas is removed, the  $\text{YH}_3$  does not decompose completely into metallic Y but into yttrium dihydride ( $\text{YH}_2$ ). However, the  $\text{YH}_2$  is a metallic phase and does therefore also exhibit LSPR. After this first irreversible cycle, the switching between metallic  $\text{YH}_2$  and insulating  $\text{YH}_3$  is fully reversible. The authors predict that yttrium nanostructures can form a crucial building block in the realization of a variety of novel

hydrogen-enabled plasmonic switching schemes. Possible applications include switchable plasmonic electromagnetically induced transparency or switchable perfect absorber devices.

**Indirect LSPR Hydrogen Sensors.** In some cases, the LSPR (or optical cross section in more general terms) of a nanoentity interacting with hydrogen is by itself too weak to be practically used for hydrogen sensing. This can arise from the fact that the material is “poor” (highly damped) when it comes to supporting LSPRs, that the particles are so small that their LSPR occurs in the UV spectral range, or, as can be the case for single-particle studies using dark-field scattering spectroscopy, that they do not scatter enough light by themselves to be easily detected. In these cases, it is possible to utilize other metal nanoparticles with superior and tailored LSPR properties as sensors that probe the hydride-forming entities located in their close vicinity (few to few tens of nanometers) via their optical near fields. In this case, the LSPR nanoparticles (typically Au) desirably do not interact with hydrogen but instead act as optical antennas and signal transducers only. We call this sensing scheme *indirect* sensing.

The first reported indirect LSPR hydrogen sensors did not utilize metal hydrides as the active material but were instead based on various composite materials composed of oxides and, typically, Au nanoparticles. In this type of sensor, the peak shift signal is either induced by electron transfer from the oxide to the plasmonic Au particles, due to dissociative  $\text{H}_2$  adsorption, or by permittivity changes in the oxide. The first study was presented by Ando *et al.*<sup>36</sup> in 2004. They used an  $\text{In}_x\text{O}_y\text{N}_z$  film with a thin Au overlayer, forming Au nanoparticles after annealing, and showed that this arrangement could be used to optically detect the presence of  $\text{H}_2$  and  $\text{NO}_2$ . Following this work,

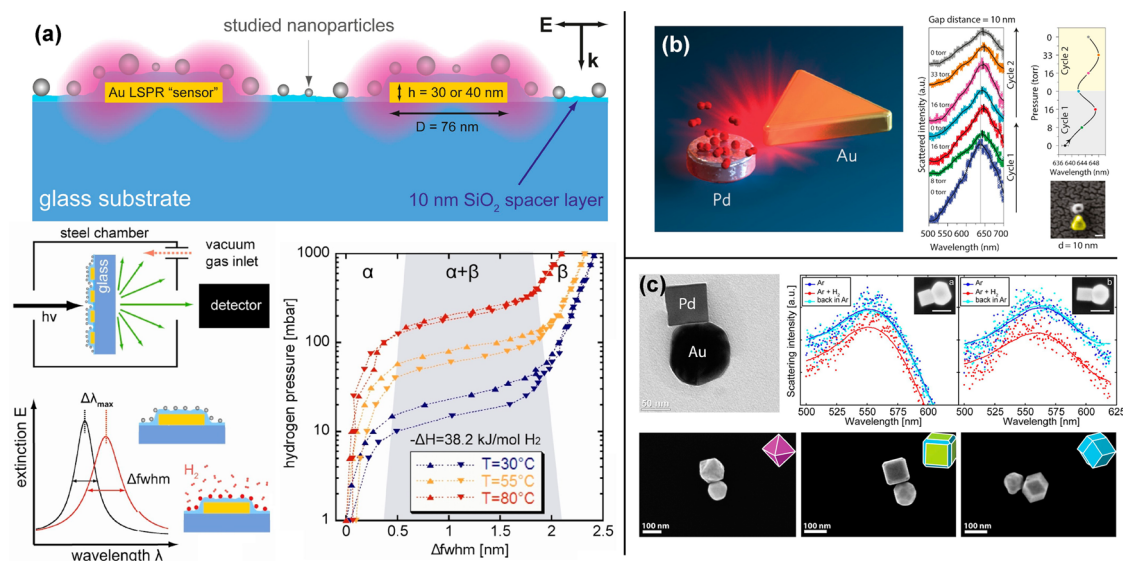


**Figure 5.** (a) Schematic illustration of the seminal indirect nanoplasmonic sensing platform used to study hydride formation and decomposition in Pd nanoparticles in the sub-10 nm size range. The plot shows optical pressure–composition isotherm measurements for 5 nm Pd nanoparticles. Adapted from ref 46. Copyright 2010 American Chemical Society. (b) Single-particle dark-field scattering spectroscopy measurements of the hydride formation and decomposition in an individual Pd disk via a tailored adjacent Au nanoantenna. Reprinted by permission from ref 51. Copyright 2011 Macmillan Publishers Ltd. (c) Heterodimer nanostructures consisting of a single-crystalline Pd nanocube attached to a spherical Au nanoparticle. The shape and surface facets of the Pd crystal can be controlled during synthesis, and the attached Au nanoparticle antenna allows for single-particle readout of hydrogen uptake in the adjacent Pd nanoparticle by means of dark-field scattering spectroscopy. Adapted from ref 64. Copyright 2014 American Chemical Society.

various oxides with embedded Au nanoparticles have been evaluated, including  $\text{In}_x\text{O}_y\text{N}_z$ ,<sup>36,37</sup>  $\text{NiO}$ ,<sup>38,39</sup>  $\text{TiO}_2$ ,<sup>40,41</sup> yttria-stabilized zirconia (YSZ),<sup>42,43</sup>  $\text{ZrTiO}_4$ ,<sup>44</sup> and  $\text{CeO}_2$ .<sup>45</sup>

The idea to utilize indirect LSPR sensors for metal hydride-based optical hydrogen sensing was introduced by Langhammer *et al.*<sup>46</sup> after having previously been successfully used to study catalytic reactions.<sup>47</sup> Figure 5a shows the indirect nanoplasmonic sensing (INPS) platform applied to study hydrogen sorption in sub-10 nm Pd particles grown on the sensor surface. The INPS platform has, since its introduction, been used for detailed studies regarding the effect of nanosizing on the hydrogen interactions with Pd nanoparticles in the sub-10 nm size range. These studies include both the thermodynamics<sup>46,48,49</sup> and the kinetics<sup>50</sup> of the hydride formation and decomposition process and have contributed to reach a deeper understanding of how the size of nanoparticles affects their hydrogen storage properties.

Other ways to study these types of systems include volumetric methods (change in gas pressure), gravimetric methods (change in mass of the system), or X-ray diffraction (change in lattice parameter). All these methods, however, require relatively large sample volumes, and they therefore suffer from problems related to the wide size distributions of the probed particles and related inhomogeneous sample material effects. To completely overcome such limiting factors, it is therefore beneficial if the hydrogenation measurements are carried out at the *single*-nanoparticle level.

Single-particle experiments would, moreover, provide the possibility to characterize the studied particle in detail, making it possible to correlate any observed effects in hydrogenation behavior to particle size, shape, and most abundant surface facets. It turns out that the indirect LSPR-sensing concept, that is, placing a plasmonic antenna adjacent to a hydride-forming entity, makes it possible to achieve single-particle hydrogen-sensing experiments. In fact, it is experimentally relatively straightforward, as only an optical dark-field microscope is needed to illuminate and collect the scattered light from the nanoparticle of interest. The first successful indirect hydrogen-sensing experiment on a single Pd nanoparticle was carried out by Liu *et al.*<sup>51</sup> Using e-beam lithography, they fabricated rectangular and triangular Au nanoantennas with a Pd nanodisk at one of its tips, in a so-called nanofocus (see Figure 5b). By tracking the LSPR scattering peak when the sample was exposed to  $\text{N}_2$  atmospheres containing various concentrations of  $\text{H}_2$  gas, they were able to monitor the hydride formation in the single Pd disk. A similar approach but using a different sample configuration was presented by Shegai *et al.*<sup>52</sup> They used a stacked arrangement of Au nanoantennas, a dielectric spacer layer, and then the hydride former (Pd or Mg) on top. In their study, they went one step further as they were able to measure complete optical pressure–composition isotherms at different temperatures and derive the enthalpy of hydride formation. Both of these works thus convincingly showed that it indeed is possible to study hydrogen uptake in single nanoentities.



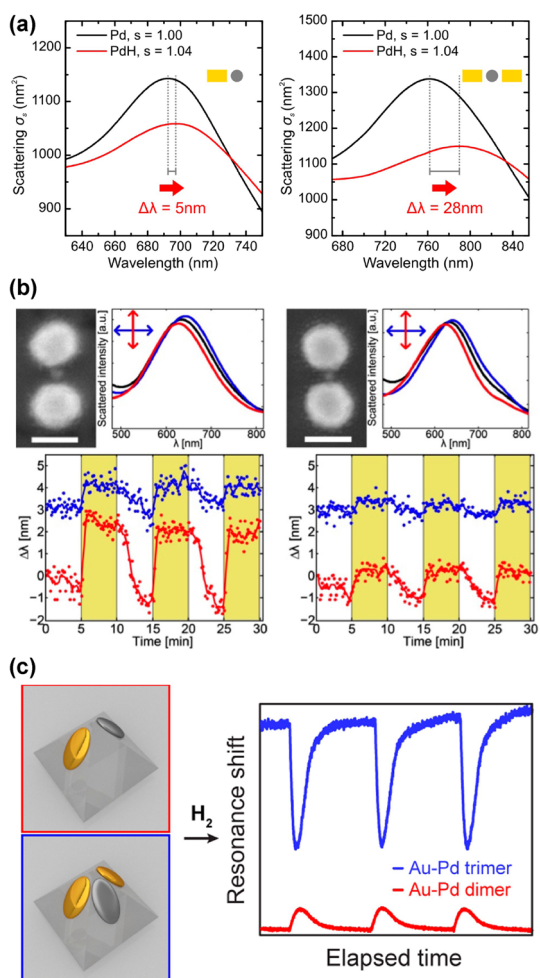


**Figure 6.** (a) Calculated changes in scattering spectra for a Pd nanodisk with either one or two plasmonic Au nanowire antennas placed in close proximity. The total observed spectral shift of the resonance peak is greatly enhanced by the addition of the second wire antenna element. Reprinted with permission from ref 55. Copyright 2012 Optical Society of America. (b) Hydride formation in single Pd nanoparticles (26 and 16 nm diameter, respectively) placed in the hot spot of a Au dimer nanoantenna structure studied using dark-field scattering spectroscopy. Scale bars in SEM images correspond to 100 nm. Adapted from ref 57. Copyright 2014 American Chemical Society. (c) Hydrogen sensing using Au–Pd dimers and trimers fabricated with reconstructable mask lithography. The trimer structure shows an enhanced signal compared to the dimer structure. Adapted from ref 58. Copyright 2014 American Chemical Society.

In both of the above cases, however, the hydride-forming Pd and Mg nanoparticles under scrutiny were relatively large (30–60 nm). As has been shown in previous studies on ensembles of particles, the interesting regime where one expects effects imposed by the particle size to become appreciable is below 10 nm.<sup>16,53,54</sup> To be able to study such small particles individually, careful considerations have to be taken on the design of the antenna structure. One way to increase the sensitivity, as presented theoretically by Tittel *et al.*<sup>55</sup> and Dasgupta *et al.*,<sup>56</sup> is to place the hydride-forming particle in the gap between two plasmonic antenna elements (Figure 6a). In this

configuration, coupling of the LSPRs in the two sensor elements will give rise to a region with a focused field (“hot spot”) in the gap between them and consequent higher sensitivity. The feasibility of this approach was recently demonstrated experimentally by Syrenova *et al.*,<sup>57</sup> where an antenna structure consisting of a Au nanodisk dimer with a small Pd particle in the gap was used to detect hydrogen uptake in a single Pd particle with a diameter of only 16 nm at a thickness of 10 nm (Figure 6b). These efforts move single-particle studies closer toward the interesting sub-10 nm size regime. Along the same lines, Yang *et al.*<sup>58</sup> also report on the benefit of having several sensor elements. They present reconstructable mask lithography with which they can produce large areas covered by Au–Pd hetero-oligomers (Figure 6c) and show both experimentally for an ensemble and theoretically for a single oligomer the difference in terms of sensitivity between a dimer and a trimer structure used for hydrogen sensing.

All previously cited experimental studies on single particles have dealt with particles that were fabricated using nanolithography techniques. This fabrication strategy was chosen because it typically provides very good control of the sensor/antenna structure and localizes them on a surface. However, when it comes to the structure and size of the hydride-forming particle, one is somewhat limited as only particles produced using physical vapor deposition methods are accessible. These particles grow with only limited control over shape and crystallinity, that is, they are typically polycrystalline. In addition, sub-10 nm size resolution is very difficult to achieve. Therefore, it is desirable to combine nanolithography-based fabrication efforts with particles synthesized with better control of the size, shape, and crystallinity parameters. One way to do this is to synthesize particles that react with hydrogen and also feature sufficiently good plasmonic properties to be able to be observed in a dark-field microscope. Tang *et al.*<sup>59</sup> synthesized Au–Pd core–shell nanoparticles that fulfill both of these criteria. They were thus able to control the shape of the synthesized particles and observed differences in particle hydrogen uptake trajectories for individual particles with different shapes, faceting, and Pd shell thickness. Interesting Au–Pd core–shell nanoparticles were also investigated for their hydrogen sorption properties by Chiu *et al.*,<sup>60,61</sup> however, at the ensemble level in aqueous solution. They were able to synthesize tetrahedral, octahedral, and cubic nanocrystals by the use of polyhedral gold nanocrystal cores and subsequent epitaxial overgrowth of a Pd shell. As they show, their approach enables the detection of hydrogen at low concentrations on the basis of the very large spectral red shifts observed for the Au–Pd nanocrystals upon exposure to dissolved hydrogen in water. The use of Au–Pd octahedra with thin Pd shells resulted in

a visually detectable change in the color of the solution within 1 min upon exposure to hydrogen.

Another interesting alternative to using a hydride-forming shell of a metal around a Au plasmonic sensor core is to *attach* the plasmonic sensor particle to the hydride former of interest. A first step in this direction was taken by Tittl *et al.*,<sup>62</sup> who synthesized Au–SiO<sub>2</sub> core–shell structures<sup>63</sup> and dispersed them on a continuous Pd film where they acted as local plasmonic “smart dust” probes. By studying the scattering from these Au–SiO<sub>2</sub> antennas, they could monitor the hydrogen uptake and release in the Pd film at the individual smart dust particle level. Based on this proof-of-principle, the authors predict that, by combining their approach with two-dimensional imaging and spectroscopic techniques, synchronized mapping and chemical sensing on several smart dust particles in parallel can be achieved.

Taking this idea one step further, Gschneidner *et al.*<sup>64</sup> have developed a method that enables finely tuned electrostatic self-assembly mediated attachment of plasmonically active nanoparticles (Au or Ag)

to shape-selected wet-chemically synthesized Pd nanoparticles with shapes such as cube, octahedron, or dodecahedron to form heterodimers. This approach has the particular advantage that the hydride former is kept pristine as it is not grown onto another material as in a core–shell structure. In this way, unwanted strain effects due to, for example, lattice-mismatch between a hydride-forming shell and a plasmonic antenna core can be avoided. Figure 5c shows examples of the achieved structures together with single-particle dark-field scattering spectral response for two different particles as they are exposed to hydrogen gas.

**Hybrid Concepts with Alternative Readouts.** As mentioned in the introduction, the traditional readout from plasmonic hydrogen sensors is a spectral shift of the resonance peak induced by hydrogen sorption in the active material. However, in two examples of “hybrid” sensing concepts, which are not strictly “direct” or “indirect” by design, alternative readout has been demonstrated. The first elegant example is the perfect absorber introduced by Tittl *et al.*<sup>65</sup> (Figure 7a). In this work, Pd nanowires were nanofabricated on top

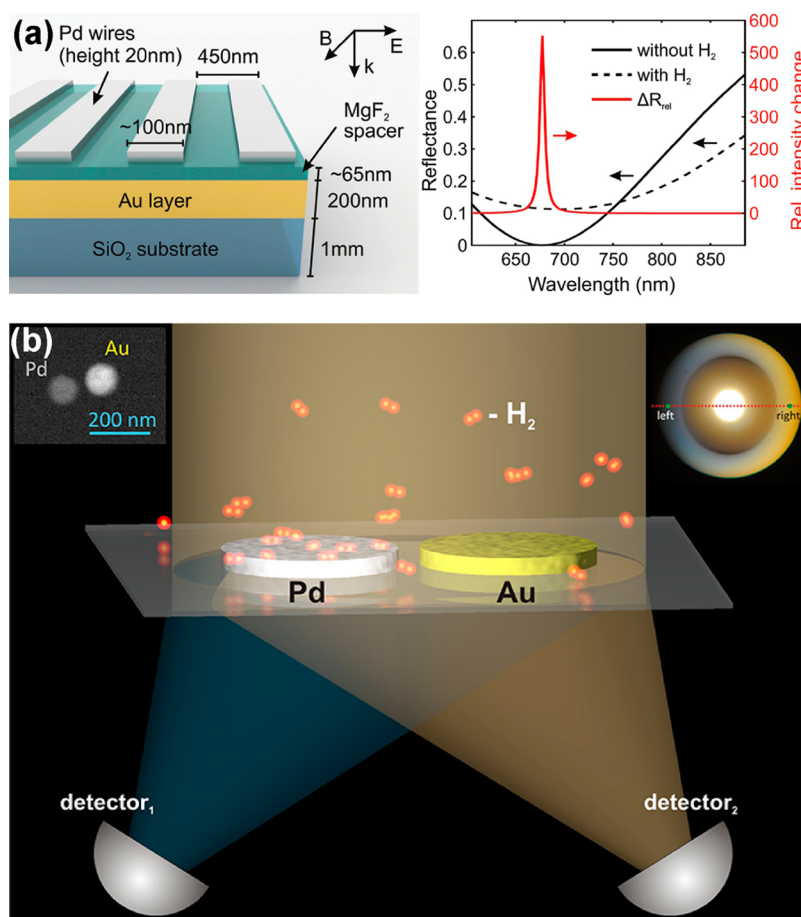


Figure 7. (a) Hydrogen sensor based on perfect absorption. The sensor is designed such that at a specific wavelength total light absorption occurs. As the sensor is exposed to hydrogen, the condition for perfect absorption is altered by the change of the dielectric properties of the Pd in the system, and the sensor starts to reflect light. Adapted from ref 65. Copyright 2011 American Chemical Society. (b) Directional light scattering at different wavelengths (“color routing”) from an ensemble of Au–Pd nanodisk heterodimer nanostructures used for hydrogen sensing by reading out the hydrogen concentration-dependent ratio of light scattered to the right and to the left. Reprinted from ref 66. Copyright 2012 American Chemical Society.

of a Au film covered by a MgF<sub>2</sub> spacer layer. Given that the geometry and material arrangements in the sample are chosen correctly, it is possible to achieve such a structure that exhibits almost perfect absorption of a specific wavelength of light. The sensing function is then provided by the effect that, as hydrogen is absorbed into the Pd nanowires, the condition for the perfect absorption is no longer perfectly fulfilled and more light is reflected from the sample surface (*i.e.*, no longer perfectly absorbed). By measuring reflection at the single wavelength where perfect absorption occurs, it is thus possible to detect the presence of hydrogen with high sensitivity. The single-wavelength readout of a simple reflectivity change is attractive for a real sensor device as it can be achieved with very simple optics, that is, without the need for a spectrometer.

Another example of an alternative plasmonic hydrogen-sensing strategy with self-referenced single-wavelength readout is the work by Shegai *et al.*,<sup>66</sup> who used a nanoplasmonic directional color routing scheme occurring in heterodimer nanostructures consisting of a Au and a Pd nanodisk element (Figure 7b). The technique is based on another work by Shegai *et al.*,<sup>67</sup> where they showed that nanodisk heterodimers can be designed in such a way that blue and red light is scattered in different spatial directions. The details of this color routing effect depend on the chosen materials of the two nanodisk elements in the heterodimer and the phase shifts between them. Hence, in the case of the Au–Pd heterostructure used for hydrogen sensing,

as hydrogen is absorbed into the Pd disk, the directional scattering effect changes and the presence of hydrogen is detected as a change in intensity scattered to the left and to the right. The single-wavelength operation capability of this approach provides the same potential advantages for real devices as in the case of the perfect absorber described above.

### SPR METAL HYDRIDE DIRECT AND INDIRECT HYDROGEN SENSORS

The main three ways to couple light into a metal film to excite an SPR mode are (i) coupling with a prism, (ii) coupling with a grating, or (iii) using an optical waveguide,<sup>24</sup> as summarized in Figure 8a. All SPR-based hydrogen sensors work in principle in the same way and differ only in how the SPR is excited. The first hydrogen sensor based on SPR was demonstrated by Chadwick *et al.*<sup>68</sup> in 1993 and was based on the excitation of SPRs in a Pd film using a prism, in conceptual agreement with the direct sensing approach. Since then, several works on SPRs in Pd have been presented using various ways for excitation: prism,<sup>69,70</sup> grating,<sup>71</sup> and waveguides.<sup>72–74</sup> It is also worth mentioning the work by Konopsky *et al.*,<sup>75</sup> where they used surface waves on a photonic crystal coupled by a prism to study the hydride formation and decomposition in Pd nanoparticles in the sub-10 nm size range and found that the sign of the signal they observe depends on the studied particle size. From this observation, they conclude that no phase transition between metallic and

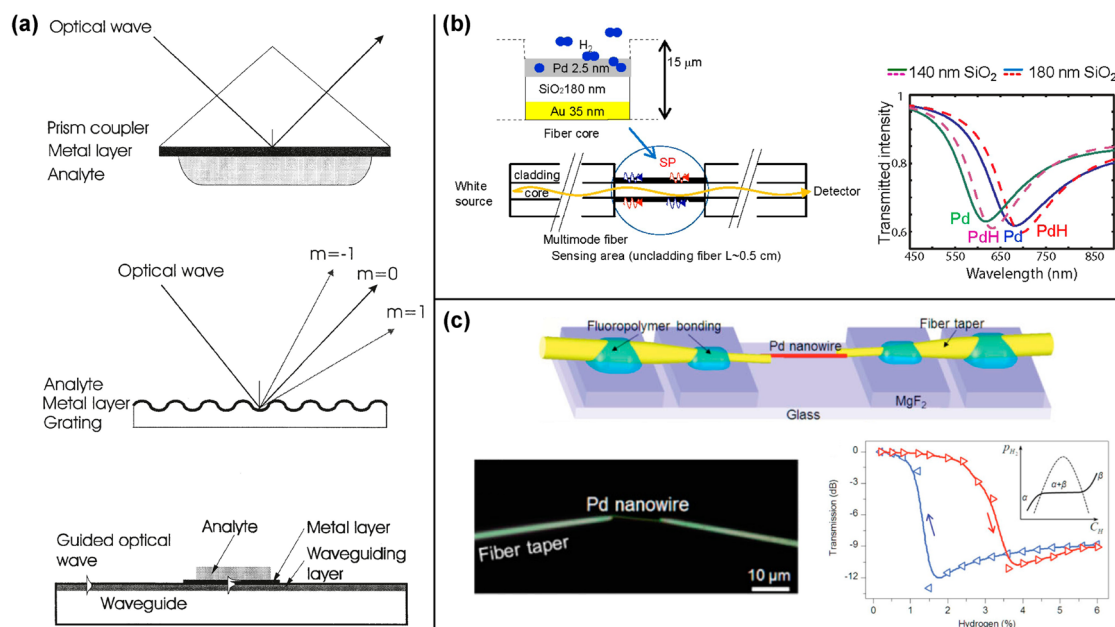


**Figure 8.** (a) Different ways to couple light to an SPR mode: prism coupling, grating coupling, or using a waveguide. Reprinted with permission from ref 24. Copyright 1999 Elsevier. (b) Optical fiber-based SPR hydrogen sensor. Part of the cladding of the fiber is replaced with an active layer, and as this layer is exposed to hydrogen and transformed into the hydride phase, the intensity of light transmitted through the fiber is changing and detected. Reproduced with permission from ref 82. Copyright 2013 Optical Society of America. (c) Measurement of the hydrogen uptake and release in a single Pd nanowire obtained by tracking the excitation of an SPR mode propagating along the nanowire. Adapted with permission from ref 92. Copyright 2013 Wiley-VCH Verlag GmbH & Co. KGaA, Weinheim.

hydride state takes place for Pd nanoparticles smaller than 2 nm.

A very practical type of SPR-based hydrogen sensor for remote sensing is based on optical fibers. They can be produced by simply removing the cladding of a section of the optical fiber and adding a material that interacts with hydrogen (often Pd) to the exposed section (see Figure 8b). In this way, the light passing through the fiber excites an SPR mode in the film, which in turn will affect the transmitted light intensity. This type of sensor was first presented by Bevenot *et al.*<sup>76</sup> Since their introduction, research into increasing the sensitivity of fiber SPR hydrogen sensors has yielded several avenues, including tapering the fiber<sup>77,78</sup> or exchanging the Pd film for multilayer structures consisting of a bottom layer with better SPR properties (*e.g.*, Au or Ag) and a top Pd film separated by a dielectric spacer layer<sup>79–83</sup> (see Figure 8b), in resemblance to the indirect LSPR sensors relying on nanoparticles.

In the framework of SPR-based hydrogen sensors, very important investigations to overcome some of the inherent problems with using Pd as the active hydrogen-sensing material are ongoing (we note here that the same inherent problems also apply to LSPR sensors based on Pd as active material). These problems arise (i) due to cross-sensitivity or poisoning of the Pd by other gases like, for example, carbon monoxide, and (ii) due to the hysteresis exhibited by Pd during the hydride formation/decomposition (see Figure 4a). Because of this hysteresis, it is not possible to get a one-to-one relationship between the sensor signal and the hydrogen concentration in the gas because the response of the sensor will depend on whether the hydrogen content has been increasing or decreasing; that is, it will depend on the history of the concentration. Both the hysteresis problem and the cross-sensitivity and poisoning of the sensor need to be eliminated (or at least reduced) if a sensor is to be of practical use. One avenue that is being explored is the possibility to alloy Pd with other metals. Chadwick *et al.*<sup>84</sup> investigated an SPR sensor based on a Pd/Ni alloy film to see if this alloy could better resist poisoning by CO and CH<sub>4</sub>. Other Pd alloys, such as Pd/Ag<sup>85</sup> and Pd/Au,<sup>86,87</sup> have also been investigated for optical-fiber-based SPR sensors due to their increased sensitivity at lower hydrogen concentrations and due to smaller hysteresis between hydride formation and decomposition.<sup>20</sup> Apart from Pd-based sensors, hydrogen-sensing layers consisting of ITO,<sup>88</sup> WO<sub>3</sub><sup>89</sup> or WO<sub>3</sub>/Pt composite films<sup>90</sup> have also been reported.

In all of the above cases, the SPR is excited in a thin film. However, SPR can also be excited along extended nano-objects such as nanowires. Interesting examples of this strategy applied to hydrogen sensing are the works by Gu *et al.*, where they study hydrogen uptake in single nanowires. They show that by using two

tapered optical fibers they are able to excite and readout the SPR mode propagating along a single Pd-coated Ag nanowire,<sup>91</sup> Pd nanowire, or Pd/Au alloy nanowire,<sup>92</sup> as summarized in Figure 8c. By changing the hydrogen partial pressure in the gas they can in this way elegantly measure hydrogen absorption and desorption isotherms for the single nanowire, reminiscent of the single-nanoparticle studies performed using dark field scattering spectroscopy.

#### ALTERNATIVE OPTICAL AND PLASMONIC HYDROGEN-SENSING APPROACHES

The changes in the optical properties of metals as they form hydrides are not only utilized in plasmonic hydrogen sensors. Alternative optical hydrogen-sensing concepts also make use of this fact. Here we chose to highlight some of the very interesting efforts in this area because they might prove to be inspirational for the plasmonic hydrogen-sensing field.

A number of sensors that rely on the change in reflection or transmission of light from/through a metal film as a hydride is formed have been developed. A recent example of such a sensor structure was presented by Ngene *et al.*,<sup>93</sup> who used the hydride formation in a Pd-capped yttrium film as the sensing reaction. As illustrated in Figure 9a, by elegantly optimizing interference effects, with these sensors, it is possible to detect the formation of the hydride by the naked eye through a distinct color change of the film, circumventing the need for electronics and external digital readouts. Moreover, as they discuss, the ability to fabricate such devices on cheap substrates such as plastics and paper makes them appealing for disposable one-time-use hydrogen sensor applications. They also demonstrate how surface modifications such as a thin layer of PTFE on top of the hydride former drastically improve the performance of their H<sub>2</sub> detector in humid and oxygen-rich environment. Therefore, the device has the potential to be used for chemical and also biochemical/biomedical H<sub>2</sub>-sensing applications such as breath hydrogen tests. At a more general level, their surface modification approach points out an interesting generic strategy for how to improve hydrogen sensors based on metal hydrides, as detailed in another recent work by Ngene *et al.*<sup>94</sup> In this second study, they investigated the effect of a thin PTFE coating on a Pd-catalyzed hydrogen sensor and observe a greatly enhanced response time of sensors with this coating compared to without.

Similarly, thin-film-based devices can also be produced on the tip of an optical fiber, which provides an easy way to introduce the sensor into the desired environment while, at the same time, carrying out a reflection measurement. These kinds of optical fiber tip sensors were first introduced by Butler<sup>95</sup> and have since then matured greatly, as illustrated by the work

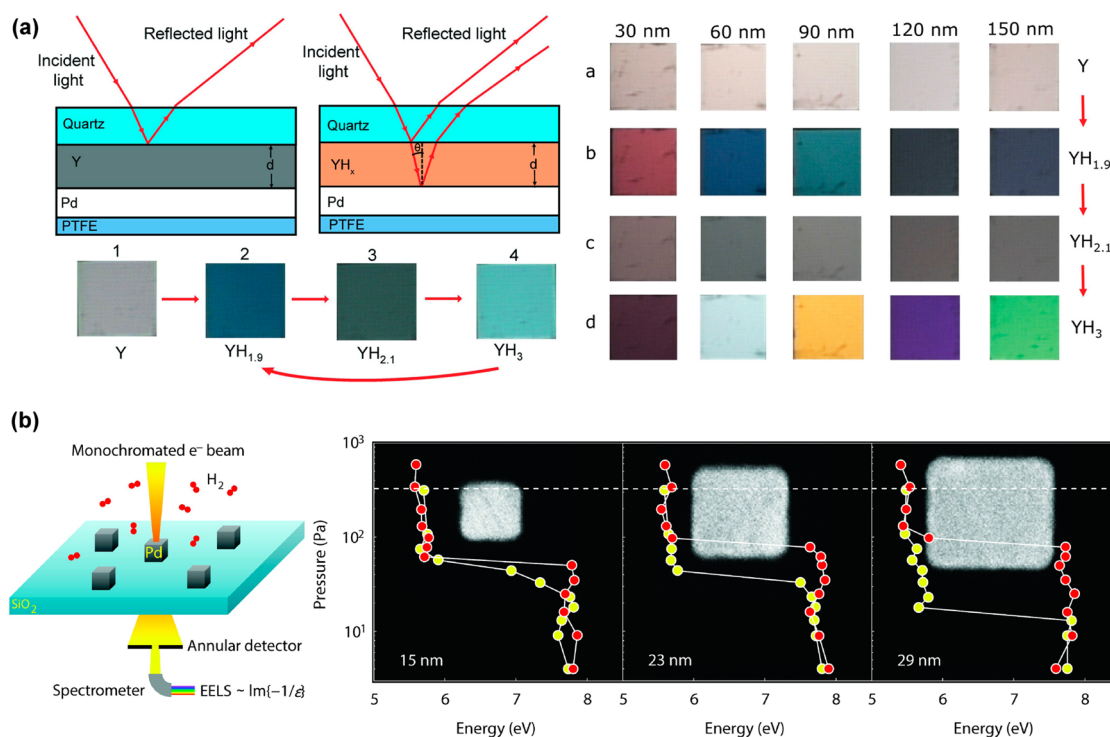


**Figure 9.** (a) Eye-readable optical hydrogen sensors based on interference in thin Y films. As the film is transformed to various hydride states, its optical properties change, which induces a change in the interference conditions and therefore a change of the perceived color of the sensor. The effect can be engineered by tailoring the thickness of the Y film. Adapted with permission from ref 93. Copyright 2013 Wiley-VCH Verlag GmbH & Co. KGaA, Weinheim. (b) Hydrogen absorption and desorption isotherms for individual single-crystalline Pd nanocubes measured in an environmental transmission electron microscope used to excite and readout energy shifts of plasmon modes in the Pd cubes by electron energy loss spectroscopy. Adapted by permission from ref 99. Copyright 2014 Macmillan Publishers Ltd.

by Slaman *et al.*,<sup>96,97</sup> where magnesium-based alloys were used.

As the final two examples, we highlight two recent studies of the hydride formation in wet-chemically synthesized Pd nanocubes. The first one was presented by Bardhan *et al.*,<sup>98</sup> who relied on monitoring changes in the luminescence intensity, proportional to the hydrogen concentration as they propose, from Pd nanocubes illuminated by a laser to investigate the hydride formation thermodynamics and kinetics of ensembles of Pd nanocubes of different sizes. The same system of Pd nanocubes was then also studied at the single-particle level by Baldi *et al.*<sup>99</sup> (Figure 9b). In their work, *in situ* electron energy loss spectroscopy is used to excite and track the plasmon resonance of individual Pd nanocubes in an environmental transmission electron microscope, where the particles can be exposed to hydrogen gas in the few millibar pressure range. In this way, by tracking shifts of the bulk plasmon resonance excited by the irradiated focused electron beam, Baldi *et al.* were able to measure isotherms of individual Pd nanocubes in the sub-30 nm size range down to 13 nm and find a size-dependent width of the hysteresis between hydrogen sorption and desorption. They explain this effect in terms of lattice strain induced in the particle by excess hydrogen in a 1 nm thin surface shell, which suppresses the two-phase coexistence typically observed in bulk Pd–H systems. The elegance

of their approach lies in the fact that they are able to structurally characterize their specimen by means of transmission electron microscopy and, at the same time, characterize its hydrogen sorption characteristics in the same instrument with single-particle resolution.

## CONCLUSIONS

Plasmonic hydrogen sensors demonstrate significant potential to both help advance our understanding of metal–hydrogen interactions at the nanoscale and as a future technical solution for hydrogen detection in a hydrogen economy, in the chemical industry, as well as in health care and food industry. They utilize SPR/LSPR excitations as the signal transducer for all-optical readout by tracking shifts or intensity changes of the plasmonic scattering or extinction “peaks”. This working principle constitutes one of the concepts' main advantages since it is risk-free to use in flammable and explosive hydrogen environments as no sparks can be generated by the all-optical readout, in stark contrast to electrical readout solutions. Another key advantage of plasmonic hydrogen sensors is the demonstrated potential for sensor miniaturization down to the single-nanoparticle level. This unique possibility has been proven to be of relevance also from a materials science perspective when it comes to the use of plasmonic hydrogen sensors in fundamental studies with the

purpose of generating deeper understanding of hydride formation processes in metal nanoparticles. The key point of such single-particle experiments is the efficient complete elimination of ensemble-averaging effects and artifacts in the material response to hydrogen, which is very difficult to achieve with other experimental techniques, especially without the need for low temperatures or low pressures.

When it comes to the use of the sensors for gas-sensing applications, to date, SPR-based sensors are more mature than their LSPR-based counterparts. However, for the latter type, during the past 5 years, a large number of different solutions and arrangements that exploit plasmonic nanostructures consisting of different materials, shapes, and sizes have been presented. To further advance these concepts, we foresee that theoretical modeling has an important role to play in suggesting future directions for optimized sensor nanostructure design for improved sensitivity. This is to some extent already happening, as exemplified on the plasmonic dimer sensor structures proposed by Tittel *et al.*<sup>55</sup> and later verified by Syrenova *et al.*<sup>57</sup> and on the work by Kumar *et al.*,<sup>100</sup> who theoretically suggest Pd adjoined split-ring resonators for superior sensitivity plasmonic hydrogen sensors.

A more general look into the future, in our opinion, sees significant efforts in the direction of sensor stability and selectivity to make it possible for SPR- and LSPR-based hydrogen sensors to reach commercial applications. This means that issues like long-term stability and cyclability, cross-sensitivity to other gas species present in the sampled gas, as well as protection from poisoning of the active sensor material by molecular species present in the sensor's working environment have to be addressed. Fortunately, efforts in this direction in related fields where metal hydrides are used as active material for hydrogen detection show that many of these problems can be overcome by the use of alloys instead of Pd as active material and by applying different types of coatings to prevent the poisoning species from reaching the active material. Therefore, it is of critical importance to get inspired by these efforts and to test and implement such concepts also in nanoplasmonic hydrogen sensors to take them to the next level and closer to real applications. The engineering of hysteresis during hydride formation to eliminate/minimize sensor readouts that depend on the history of the sensor is another challenge that has to be tackled, for example, by engineering the properties of the active material in the sensor by alloying with other elements. Finally, we also want to note that more focus should be put on the improvement of sensor resolution and detection limits in the low hydrogen concentration regime. Specifically, this means to focus efforts toward the detection of hydrogen concentrations at levels where the common active material Pd does not form a hydride at ambient conditions and thus remains in the

$\alpha$ -phase where both volume expansion and changes in the dielectric properties of Pd are very small.

**Conflict of Interest:** The authors declare no competing financial interest.

**Acknowledgment.** We acknowledge the Swedish Research Council Project 2010-4041, the Swedish Foundation for Strategic Research Framework Program RMA11-0037, and the Chalmers Area of Advance Nanoscience and Nanotechnology.

## REFERENCES AND NOTES

- Züttel, A.; Borgschulte, A.; Schlapbach, L. *Hydrogen as a Future Energy Carrier*; Wiley-VCH: Weinheim, Germany, 2008.
- Schlapbach, L. Technology: Hydrogen-Fuelled Vehicles. *Nature* **2009**, *460*, 809–811.
- Gupta, R. B. *Hydrogen Fuel: Production, Transport and Storage*; CRC Press: Boca Raton, FL, 2009.
- Wilkins, J. R.; Stoner, G. E.; Boykin, E. H. Microbial Detection Method Based on Sensing Molecular-Hydrogen. *Appl. Microbiol.* **1974**, *27*, 949–952.
- Hitchcock, C. H. S. Determination of Hydrogen as a Marker in Irradiated Frozen Food. *J. Sci. Food Agric.* **2000**, *80*, 131–136.
- Hurme, E. U.; Ahvenainen, R. A Nondestructive Leak Detection Method for Flexible Food Packages Using Hydrogen as a Tracer Gas. *J. Food Prot.* **1998**, *61*, 1165–1169.
- Shin, W. Medical Applications of Breath Hydrogen Measurements. *Anal. Bioanal. Chem.* **2014**, 1–9.
- Buttner, W. J.; Post, M. B.; Burgess, R.; Rivkin, C. An Overview of Hydrogen Safety Sensors and Requirements. *Int. J. Hydrogen Energy* **2011**, *36*, 2462–2470.
- Boon-Brett, L.; Bousek, J.; Black, G.; Moretto, P.; Castello, P.; Hubert, T.; Banach, U. Identifying Performance Gaps in Hydrogen Safety Sensor Technology for Automotive and Stationary Applications. *Int. J. Hydrogen Energy* **2010**, *35*, 373–384.
- Hubert, T.; Boon-Brett, L.; Black, G.; Banach, U. Hydrogen Sensors—A Review. *Sens. Actuators, B* **2011**, *157*, 329–352.
- Ando, M. Recent Advances in Optochemical Sensors for the Detection of H<sub>2</sub>, O<sub>2</sub>, O<sub>3</sub>, CO, CO<sub>2</sub> and H<sub>2</sub>O in Air. *Trends Anal. Chem.* **2006**, *25*, 937–948.
- Fukai, Y. *The Metal–Hydrogen System*, 2nd ed.; Springer-Verlag: Berlin, 2005.
- Schlapbach, L.; Züttel, A. Hydrogen-Storage Materials for Mobile Applications. *Nature* **2001**, *414*, 353–358.
- Toyota Fuel Cell Vehicle. [http://www.toyota-global.com/innovation/environmental\\_technology/fuelcell\\_vehicle/](http://www.toyota-global.com/innovation/environmental_technology/fuelcell_vehicle/).
- Oumellal, Y.; Rougier, A.; Nazri, G. A.; Tarascon, J. M.; Aymard, L. Metal Hydrides for Lithium-Ion Batteries. *Nat. Mater.* **2008**, *7*, 916–921.
- Berube, V.; Radtke, G.; Dresselhaus, M.; Chen, G. Size Effects on the Hydrogen Storage Properties of Nanostructured Metal Hydrides: A Review. *Int. J. Energy Res.* **2007**, *31*, 637–663.
- Schwarz, R. B.; Khachatryan, A. G. Thermodynamics of Open Two-Phase Systems with Coherent Interfaces: Application to Metal-Hydrogen Systems. *Acta Mater.* **2006**, *54*, 313–323.
- Hughes, R. C.; Schubert, W. K.; Zipperian, T. E.; Rodriguez, J. L.; Plut, T. A. Thin-Film Palladium and Silver Alloys and Layers for Metal-Insulator-Semiconductor Sensors. *J. Appl. Phys.* **1987**, *62*, 1074–1083.
- Hughes, R. C.; Schubert, W. K. Thin Films of Pd/Ni Alloys for Detection of High Hydrogen Concentrations. *J. Appl. Phys.* **1992**, *71*, 542–544.
- Westerwaal, R. J.; Rooijmans, J. S. A.; Leclercq, L.; Gheorghie, D. G.; Radeva, T.; Mooij, L.; Mak, T.; Polak, L.; Slaman, M.; Dam, B.; Rasing, T. Nanostructured Pd–Au Based Fiber Optic Sensors for Probing Hydrogen Concentrations in Gas Mixtures. *Int. J. Hydrogen Energy* **2013**, *38*, 4201–4212.

21. Wicke, E.; Brodowsky, H.; Züchner, H. Hydrogen in Palladium and Palladium Alloys. In *Hydrogen in Metals II*; Alefeld, G., Völkl, J., Eds.; Springer-Verlag: Berlin, 1978; pp 73–155.
22. Faraday, M. The Bakerian Lecture: Experimental Relations of Gold (and Other Metals) to Light. *Philos. Trans. R. Soc. London* **1857**, *147*, 145–181.
23. Kelly, K. L.; Coronado, E.; Zhao, L. L.; Schatz, G. C. The Optical Properties of Metal Nanoparticles: The Influence of Size, Shape, and Dielectric Environment. *J. Phys. Chem. B* **2003**, *107*, 668–677.
24. Homola, J.; Yee, S. S.; Gauglitz, G. Surface Plasmon Resonance Sensors: Review. *Sens. Actuators, B* **1999**, *54*, 3–15.
25. Silkin, V. M.; Muino, R. D.; Chernov, I. P.; Chulkov, E. V.; Echenique, P. M. Tuning the Plasmon Energy of Palladium–Hydrogen Systems by Varying the Hydrogen Concentration. *J. Phys.: Condens. Matter* **2012**, *24*, 104021.
26. Langhammer, C.; Zoric, I.; Kasemo, B. Hydrogen Storage in Pd Nanodisks Characterized with a Novel Nanoplasmonic Sensing Scheme. *Nano Lett.* **2007**, *7*, 3122–3127.
27. Zoric, I.; Larsson, E. M.; Kasemo, B.; Langhammer, C. Localized Surface Plasmons Shed Light on Nanoscale Metal Hydrides. *Adv. Mater.* **2010**, *22*, 4628–4633.
28. Larsson, E. M.; Edvardsson, M. E. M.; Langhammer, C.; Zoric, I.; Kasemo, B. A Combined Nanoplasmonic and Electrodeless Quartz Crystal Microbalance Setup. *Rev. Sci. Instrum.* **2009**, *80*, 125105.
29. Poyli, M. A.; Silkin, V. M.; Chernov, I. P.; Echenique, P. M.; Muino, R. D.; Aizpurua, J. Multiscale Theoretical Modeling of Plasmonic Sensing of Hydrogen Uptake in Palladium Nanodisks. *J. Phys. Chem. Lett.* **2012**, *3*, 2556–2561.
30. Langhammer, C.; Larsson, E. M.; Zhdanov, V. P.; Zoric, I. Asymmetric Hysteresis in Nanoscopic Single-Metal Hydrides: Palladium Nanorings. *J. Phys. Chem. C* **2012**, *116*, 21201–21207.
31. Niu, W. X.; Zhang, W. Q.; Firdoz, S.; Lu, X. M. Controlled Synthesis of Palladium Concave Nanocubes with Sub-10-Nanometer Edges and Corners for Tunable Plasmonic Property. *Chem. Mater.* **2014**, *26*, 2180–2186.
32. Strohfeldt, N.; Tittel, A.; Giessen, H. Long-Term Stability of Capped and Buffered Palladium-Nickel Thin Films and Nanostructures for Plasmonic Hydrogen Sensing Applications. *Opt. Mater. Express* **2013**, *3*, 194–204.
33. Sil, D.; Gilroy, K. D.; Niaux, A.; Boulesbaa, A.; Neretina, S.; Borguet, E. Seeing Is Believing: Hot Electron Based Gold Nanoplasmonic Optical Hydrogen Sensor. *ACS Nano* **2014**, *8*, 7755–7762.
34. Mukherjee, S.; Libisch, F.; Large, N.; Neumann, O.; Brown, L. V.; Cheng, J.; Lassiter, J. B.; Carter, E. A.; Nordlander, P.; Halas, N. J. Hot Electrons Do the Impossible: Plasmon-Induced Dissociation of H<sub>2</sub> on Au. *Nano Lett.* **2013**, *13*, 240–247.
35. Strohfeldt, N.; Tittel, A.; Schaferling, M.; Neubrech, F.; Kreibitz, U.; Griessen, R.; Giessen, H. Yttrium Hydride Nanoantennas for Active Plasmonics. *Nano Lett.* **2014**, *14*, 1140–1147.
36. Ando, M.; Steffes, H.; Chabicovsky, R.; Haruta, M.; Stangl, G. Optical and Electrical H<sub>2</sub>- and NO<sub>2</sub>-Sensing Properties of Au/InxOvNz Films. *IEEE Sens. J.* **2004**, *4*, 232–236.
37. Steffes, H.; Schleunitz, A.; Gernert, U.; Chabicovsky, R.; Obermeier, E. A Novel Optical Gas Sensor Based on Sputtered InxOyNz Films with Gold-Nano-Dots. *Microelectron. Eng.* **2006**, *83*, 1197–1200.
38. Buso, D.; Busato, G.; Guglielmi, M.; Martucci, A.; Bello, V.; Mattei, G.; Mazzoldi, P.; Post, M. L. Selective Optical Detection of H<sub>2</sub> and CO with SiO<sub>2</sub> Sol–Gel Films Containing NiO and Au Nanoparticles. *Nanotechnology* **2007**, *18*, 475505.
39. Buso, D.; Guglielmi, M.; Martucci, A.; Mattei, G.; Mazzoldi, P.; Sada, C.; Post, M. L. Growth of Cookie-like Au/NiO Nanoparticles in SiO<sub>2</sub> Sol–Gel Films and Their Optical Gas Sensing Properties. *Cryst. Growth Des.* **2008**, *8*, 744–749.
40. Buso, D.; Post, M.; Cantalini, C.; Mulvaney, P.; Martucci, A. Gold Nanoparticle-Doped TiO<sub>2</sub> Semiconductor Thin Films: Gas Sensing Properties. *Adv. Funct. Mater.* **2008**, *18*, 3843–3849.
41. Della Gaspera, E.; Bersani, M.; Mattei, G.; Nguyen, T. L.; Mulvaney, P.; Martucci, A. Cooperative Effect of Au and Pt inside TiO<sub>2</sub> Matrix for Optical Hydrogen Detection at Room Temperature Using Surface Plasmon Spectroscopy. *Nanoscale* **2012**, *4*, 5972–5979.
42. Rogers, P. H.; Sirinakis, G.; Carpenter, M. A. Direct Observations of Electrochemical Reactions within Au-YSZ Thin Films via Absorption Shifts in the an Nanoparticle Surface Plasmon Resonance. *J. Phys. Chem. C* **2008**, *112*, 6749–6757.
43. Dharmalingam, G.; Joy, N. A.; Grisafe, B.; Carpenter, M. A. Plasmonics-Based Detection of H<sub>2</sub> and CO: Discrimination between Reducing Gases Facilitated by Material Control. *Beilstein J. Nanotechnol.* **2012**, *3*, 712–721.
44. Pramanik, S.; Pal, S.; De, G. Au Nanoparticles Doped ZrTiO<sub>4</sub> Films and Hydrogen Gas Induced Au-Plasmon Shifting. *J. Mater. Chem.* **2010**, *20*, 9081–9088.
45. Joy, N. A.; Nandasiri, M. I.; Rogers, P. H.; Jiang, W. L.; Varga, T.; Kuchibhatla, S. V. N. T.; Thevuthasan, S.; Carpenter, M. A. Selective Plasmonic Gas Sensing: H<sub>2</sub>, NO<sub>2</sub>, and CO Spectral Discrimination by a Single Au-CeO<sub>2</sub> Nanocomposite Film. *Anal. Chem.* **2012**, *84*, 5025–5034.
46. Langhammer, C.; Larsson, E. M.; Kasemo, B.; Zoric, I. Indirect Nanoplasmonic Sensing: Ultrasensitive Experimental Platform for Nanomaterials Science and Optical Nanocalorimetry. *Nano Lett.* **2010**, *10*, 3529–3538.
47. Larsson, E. M.; Langhammer, C.; Zoric, I.; Kasemo, B. Nanoplasmonic Probes of Catalytic Reactions. *Science* **2009**, *326*, 1091–1094.
48. Langhammer, C.; Zhdanov, V. P.; Zoric, I.; Kasemo, B. Size-Dependent Hysteresis in the Formation and Decomposition of Hydride in Metal Nanoparticles. *Chem. Phys. Lett.* **2010**, *488*, 62–66.
49. Wadell, C.; Pingel, T.; Olsson, E.; Zorić, I.; Zhdanov, V. P.; Langhammer, C. Thermodynamics of Hydride Formation and Decomposition in Supported Sub-10 nm Pd Nanoparticles of Different Sizes. *Chem. Phys. Lett.* **2014**, *603*, 75–81.
50. Langhammer, C.; Zhdanov, V. P.; Zoric, I.; Kasemo, B. Size-Dependent Kinetics of Hydriding and Dehydriding of Pd Nanoparticles. *Phys. Rev. Lett.* **2010**, *104*, 135502.
51. Liu, N.; Tang, M. L.; Hentschel, M.; Giessen, H.; Alivisatos, A. P. Nanoantenna-Enhanced Gas Sensing in a Single Tailored Nanofocus. *Nat. Mater.* **2011**, *10*, 631–636.
52. Shegai, T.; Langhammer, C. Hydride Formation in Single Palladium and Magnesium Nanoparticles Studied by Nanoplasmonic Dark-Field Scattering Spectroscopy. *Adv. Mater.* **2011**, *23*, 4409–4414.
53. Pundt, A.; Sachs, C.; Winter, M.; Reetz, M. T.; Fritsch, D.; Kirchheim, R. Hydrogen Sorption in Elastically Soft Stabilized Pd-Clusters. *J. Alloys Compd.* **1999**, *293*, 480–483.
54. Zuttel, A.; Nutzenadel, C.; Schmid, G.; Chartouni, D.; Schlapbach, L. Pd-Cluster Size Effects of the Hydrogen Sorption Properties. *J. Alloys Compd.* **1999**, *293*, 472–475.
55. Tittel, A.; Kremers, C.; Dorfmüller, J.; Chigrin, D. N.; Giessen, H. Spectral Shifts in Optical Nanoantenna-Enhanced Hydrogen Sensors. *Opt. Mater. Express* **2012**, *2*, 111–118.
56. Dasgupta, A.; Kumar, G. V. P. Palladium Bridged Gold Nanocylinder Dimer: Plasmonic Properties and Hydrogen Sensitivity. *Appl. Opt.* **2012**, *51*, 1688–1693.
57. Syrenova, S.; Wadell, C.; Langhammer, C. Shrinking-Hole Colloidal Lithography: Self-Aligned Nanofabrication of Complex Plasmonic Nanoantennas. *Nano Lett.* **2014**, *14*, 2655–2663.
58. Yang, A. K.; Huntington, M. D.; Cardinal, M. F.; Masango, S. S.; Van Duyne, R. P.; Odom, T. W. Hetero-oligomer Nanoparticle Arrays for Plasmon-Enhanced Hydrogen Sensing. *ACS Nano* **2014**, *8*, 7639–7647.
59. Tang, M. L.; Liu, N.; Dionne, J. A.; Alivisatos, A. P. Observations of Shape-Dependent Hydrogen Uptake Trajectories from Single Nanocrystals. *J. Am. Chem. Soc.* **2011**, *133*, 13220–13223.

60. Chiu, C. Y.; Huang, M. H. Polyhedral Au–Pd Core–Shell Nanocrystals as Highly Spectrally Responsive and Reusable Hydrogen Sensors in Aqueous Solution. *Angew. Chem., Int. Ed.* **2013**, *52*, 12709–12713.
61. Chiu, C. Y.; Yang, M. Y.; Lin, F. C.; Huang, J. S.; Huang, M. H. Facile Synthesis of Au–Pd Core–Shell Nanocrystals with Systematic Shape Evolution and Tunable Size for Plasmonic Property Examination. *Nanoscale* **2014**, *6*, 7656–7665.
62. Tittl, A.; Yin, X. H.; Giessen, H.; Tian, X. D.; Tian, Z. Q.; Kremers, C.; Chigrin, D. N.; Liu, N. Plasmonic Smart Dust for Probing Local Chemical Reactions. *Nano Lett.* **2013**, *13*, 1816–1821.
63. Li, J. F.; Huang, Y. F.; Ding, Y.; Yang, Z. L.; Li, S. B.; Zhou, X. S.; Fan, F. R.; Zhang, W.; Zhou, Z. Y.; Wu, D. Y.; Ren, B.; Wang, Z. L.; Tian, Z. Q. Shell-Isolated Nanoparticle-Enhanced Raman Spectroscopy. *Nature* **2010**, *464*, 392–395.
64. Gschneidner, T. A.; Fernandez, Y. A. D.; Syrenova, S.; Westerlund, F.; Langhammer, C.; Moth-Poulsen, K. A Versatile Self-Assembly Strategy for the Synthesis of Shape-Selected Colloidal Noble Metal Nanoparticle Heterodimers. *Langmuir* **2014**, *30*, 3041–3050.
65. Tittl, A.; Mai, P.; Taubert, R.; Dregely, D.; Liu, N.; Giessen, H. Palladium-Based Plasmonic Perfect Absorber in the Visible Wavelength Range and Its Application to Hydrogen Sensing. *Nano Lett.* **2011**, *11*, 4366–4369.
66. Shegai, T.; Johansson, P.; Langhammer, C.; Kall, M. Directional Scattering and Hydrogen Sensing by Bimetallic Pd–Au Nanoantennas. *Nano Lett.* **2012**, *12*, 2464–2469.
67. Shegai, T.; Chen, S.; Miljkovic, V. D.; Zengin, G.; Johansson, P.; Kall, M. A Bimetallic Nanoantenna for Directional Colour Routing. *Nat. Commun.* **2011**, *2*, 481.
68. Chadwick, B.; Gal, M. Enhanced Optical-Detection of Hydrogen Using the Excitation of Surface-Plasmons in Palladium. *Appl. Surf. Sci.* **1993**, *68*, 135–138.
69. Konopsky, V. N.; Basmanov, D. V.; Alieva, E. V.; Dolgy, D. I.; Olshansky, E. D.; Sekatskii, S. K.; Dietler, G. Registration of Long-Range Surface Plasmon Resonance by Angle-Scanning Feedback and Its Implementation for Optical Hydrogen Sensing. *New J. Phys.* **2009**, *11*, 063049.
70. Morjan, M.; Zuchner, H.; Cammann, K. Contributions to a Reliable Hydrogen Sensor Based on Surface Plasmon Resonance Spectroscopy. *Surf. Sci.* **2009**, *603*, 1353–1359.
71. Lin, K. Q.; Lu, Y. H.; Chen, J. X.; Zheng, R. S.; Wang, P.; Ming, H. Surface Plasmon Resonance Hydrogen Sensor Based on Metallic Grating with High Sensitivity. *Opt. Express* **2008**, *16*, 18599–18604.
72. Tobiska, P.; Hugon, O.; Trouillet, A.; Gagnaire, H. An Integrated Optic Hydrogen Sensor Based on SPR on Palladium. *Sens. Actuators, B* **2001**, *74*, 168–172.
73. Fong, N. R.; Berini, P.; Tait, R. N. Modeling and Design of Hydrogen Gas Sensors Based on a Membrane-Supported Surface Plasmon Waveguide. *Sens. Actuators, B* **2012**, *161*, 285–291.
74. Alam, M. Z.; Carriere, N.; Bahrami, F.; Mojahedi, M.; Aitchison, J. S. Pd-Based Integrated Optical Hydrogen Sensor on a Silicon-on-Insulator Platform. *Opt. Lett.* **2013**, *38*, 1428–1430.
75. Konopsky, V. N.; Basmanov, D. V.; Alieva, E. V.; Sekatskii, S. K.; Dietler, G. Size-Dependent Hydrogen Uptake Behavior of Pd Nanoparticles Revealed by Photonic Crystal Surface Waves. *Appl. Phys. Lett.* **2012**, *100*, 083108.
76. Bevenot, X.; Trouillet, A.; Veillas, C.; Gagnaire, H.; Clement, M. Surface Plasmon Resonance Hydrogen Sensor Using an Optical Fibre. *Meas. Sci. Technol.* **2002**, *13*, 118–124.
77. Villatoro, J.; Luna-Moreno, D.; Monzon-Hernandez, D. Optical Fiber Hydrogen Sensor for Concentrations below the Lower Explosive Limit. *Sens. Actuators, B* **2005**, *110*, 23–27.
78. Villatoro, J.; Monzon-Hernandez, D. Fast Detection of Hydrogen with Nano Fiber Tapers Coated with Ultra Thin Palladium Layers. *Opt. Express* **2005**, *13*, 5087–5092.
79. Perrotton, C.; Javahiry, N.; Slaman, M.; Dam, B.; Meyrueis, P. Fiber Optic Surface Plasmon Resonance Sensor Based on Wavelength Modulation for Hydrogen Sensing. *Opt. Express* **2011**, *19*, A1175–A1183.
80. Bhatia, P.; Gupta, B. D. Surface Plasmon Resonance Based Fiber Optic Hydrogen Sensor Utilizing Wavelength Interrogation. *Proc. SPIE* **2012**, *8351*, 83511V.
81. Hosoki, A.; Nishiyama, M.; Igawa, H.; Seki, A.; Choi, Y.; Watanabe, K. A Surface Plasmon Resonance Hydrogen Sensor Using Au/Ta<sub>2</sub>O<sub>5</sub>/Pd Multi-layers on Hetero-core Optical Fiber Structures. *Sens. Actuators, B* **2013**, *185*, 53–58.
82. Perrotton, C.; Westerwaal, R. J.; Javahiry, N.; Slaman, M.; Schreuders, H.; Dam, B.; Meyrueis, P. A Reliable, Sensitive and Fast Optical Fiber Hydrogen Sensor Based on Surface Plasmon Resonance. *Opt. Express* **2013**, *21*, 382–390.
83. Hosoki, A.; Nishiyama, M.; Igawa, H.; Seki, A.; Watanabe, K. A Hydrogen Curing Effect on Surface Plasmon Resonance Fiber Optic Hydrogen Sensors Using an Annealed Au/Ta<sub>2</sub>O<sub>5</sub>/Pd Multi-layers Film. *Opt. Express* **2014**, *22*, 18556–18563.
84. Chadwick, B.; Tann, J.; Brungs, M.; Gal, M. A Hydrogen Sensor-Based on the Optical-Generation of Surface-Plasmons in a Palladium Alloy. *Sens. Actuators, B* **1994**, *17*, 215–220.
85. Hu, J. D.; Jiang, M.; Lin, Z. L. Novel Technology for Depositing a Pd–Ag Alloy Film on a Tapered Optical Fibre for Hydrogen Sensing. *J. Opt. A: Pure Appl. Opt.* **2005**, *7*, 593–598.
86. Luna-Moreno, D.; Monzon-Hernandez, D. Effect of the Pd–Au Thin Film Thickness Uniformity on the Performance of an Optical Fiber Hydrogen Sensor. *Appl. Surf. Sci.* **2007**, *253*, 8615–8619.
87. Luna-Moreno, D.; Monzon-Hernandez, D.; Villatoro, J.; Badenes, G. Optical Fiber Hydrogen Sensor Based on Core Diameter Mismatch and Annealed Pd–Au Thin Films. *Sens. Actuators, B* **2007**, *125*, 66–71.
88. Mishra, S. K.; Gupta, B. D. Surface Plasmon Resonance-Based Fiber-Optic Hydrogen Gas Sensor Utilizing Indium–Tin Oxide (ITO) Thin Films. *Plasmonics* **2012**, *7*, 627–632.
89. Nau, D.; Seidel, A.; Orzekowsky, R. B.; Lee, S. H.; Deb, S.; Giessen, H. Hydrogen Sensor Based on Metallic Photonic Crystal Slabs. *Opt. Lett.* **2010**, *35*, 3150–3152.
90. Wang, X. G.; Tang, Y. K.; Zhou, C. D.; Liao, B. Design and Optimization of the Optical Fiber Surface Plasmon Resonance Hydrogen Sensor Based on Wavelength Modulation. *Opt. Commun.* **2013**, *298*, 88–94.
91. Gu, F. X.; Zeng, H. P.; Tong, L. M.; Zhuang, S. L. Metal Single-Nanowire Plasmonic Sensors. *Opt. Lett.* **2013**, *38*, 1826–1828.
92. Gu, F.; Zeng, H.; Zhu, Y. B.; Yang, Q.; Ang, L. K.; Zhuang, S. Single-Crystal Pd and Its Alloy Nanowires for Plasmon Propagation and Highly Sensitive Hydrogen Detection. *Adv. Opt. Mater.* **2014**, *2*, 189–196.
93. Ngene, P.; Radeva, T.; Slaman, M.; Westerwaal, R. J.; Schreuders, H.; Dam, B. Seeing Hydrogen in Colors: Low-Cost and Highly Sensitive Eye Readable Hydrogen Detectors. *Adv. Funct. Mater.* **2013**, *2374*–2382.
94. Ngene, P.; Westerwaal, R. J.; Sachdeva, S.; Haije, W.; de Smet, L. C. P. M.; Dam, B. Polymer-Induced Surface Modifications of Pd-Based Thin Films Leading to Improved Kinetics in Hydrogen Sensing and Energy Storage Applications. *Angew. Chem., Int. Ed.* **2014**, *53*, 12081–12085.
95. Butler, M. A. Fiber Optic Sensor for Hydrogen Concentrations near the Explosive Limit. *J. Electrochem. Soc.* **1991**, *138*, L46–L47.
96. Slaman, M.; Dam, B.; Pasturel, M.; Borsa, D. M.; Schreuders, H.; Rector, J. H.; Griessen, R. Fiber Optic Hydrogen Detectors Containing Mg-Based Metal Hydrides. *Sens. Actuators, B* **2007**, *123*, 538–545.
97. Slaman, M.; Dam, B.; Schreuders, H.; Griessen, R. Optimization of Mg-Based Fiber Optic Hydrogen Detectors by Alloying the Catalyst. *Int. J. Hydrogen Energy* **2008**, *33*, 1084–1089.



98. Bardhan, R.; Hedges, L. O.; Pint, C. L.; Javey, A.; Whitlam, S.; Urban, J. J. Uncovering the Intrinsic Size Dependence of Hydriding Phase Transformations in Nanocrystals. *Nat. Mater.* **2013**, *12*, 905–912.
99. Baldi, A.; Narayan, T. C.; Koh, A. L.; Dionne, J. A. *In Situ* Detection of Hydrogen-Induced Phase Transitions in Individual Palladium Nanocrystals. *Nat. Mater.* **2014**, *13*, 1143–1148.
100. Kumar, G. V. P.; Raghuvanshi, M. Palladium Adjoined Gold Split-Ring Resonators: A Prospective Nanoplasmonic Hydrogen Sensor. *Opt. Commun.* **2013**, *300*, 65–68.